Computational Experiments on the Motion and Generation of Defects in Polymer Crystals

Bobby G. Sumpter, Donald W. Noid, and Bernhard Wunderlich*

Chemistry Division, Oak Ridge National Laboratory, Oak Ridge, Tennessee 37831-6182, and Department of Chemistry, University of Tennessee, Knoxville, Tennessee 37996-1600

Received February 27, 1992; Revised Manuscript Received June 29, 1992

ABSTRACT: Computer experiments using the molecular dynamics method have been carried out in order to investigate the formation and motion of defects in polymer crystals. The simulations were carried out on a crystal of 12.6-nm-long chains consisting of 3700 CH_2 groups over times of 20 ps, and preliminary results for crystals containing up to 30 000 atoms that include the hydrogens explicitly are discussed. Chain diffusion through the crystal is shown to involve sharply defined thermal conformational defects and longer-range soft twists. An activation energy for the formation of conformational defects is found to be on the order of 16 kJ/mol and an additional "activation" energy gradient of 4 kJ/mol is determined to be necessary to cause directed motion of a chain through the crystal. At 350 K the rate of conformational defect formation is about 10^{10} s^{-1}, causing doubling of a crystal in thickness on a time scale of 0.1 ns. Both structural and dynamical details of defect generation and motion are extracted from the extensive simulations, and the results are discussed in context to currently existing theories for lamellar thickening and relaxation behavior in polymer crystals.

Introduction

Much of the early research on crystals of macromolecules dealt with the establishment of detailed knowledge about crystal structure, morphology, and molecular macroconformation.[1] Special techniques, ranging from optical microscopy, the various forms of electron microscopy, and X-ray, neutron, and electron diffraction to the new atomic force microscopy,[2] were necessary to bridge the understanding from the visible, macroscopic, millimeter-size scale to the basic microscopic or atomic, nanometer-size scale.

More recently, it has become possible to "experiment" with motion on an atomic, picosecond time scale using supercomputers.[3] One should recognize that in the length dimensions magnifications of, at most, 10^6 are necessary to reach the atomic size; in the time dimension, in contrast, a speedup by a factor of 10^{12} is necessary to go from the human time scale to the atomic time scale.

New, more efficient computer programming[4] has permitted us to do molecular dynamics simulations of sufficiently long times for crystals of sufficient size to get a realistic super-slow motion representation of the crystal dynamics. Immediately it became obvious that thermal conformational defects of picosecond lifetime and 10^{10} s^{-1} rate of formation exist in the crystal at temperatures far below the melting point.[3,5] The defect dynamics should be linked to experiments such as solid-state NMR, quasielastic neutron scattering, and mechanical and dielectric relaxation, while the defect concentration can be checked by calorimetry and infrared analysis.

In our prior work, the vibrational state of a polyethylene-like crystal was evaluated[6] and the motion connected with the α-relaxation analyzed.[3,7] A preliminary report of some of the work presented here was given at the Materials Research Society Meeting in Boston in Dec 1990.[8] A treatise of the molecular dynamics of polymer crystals with a detailed summary of the extensive literature on defects in macromolecular crystals is in preparation.[9] In addition, the effect of external forces on crystal deformation[10,11] has been investigated and a study of the dynamics of even larger paraffin crystals of up to 30 000 atoms, including its melting, is underway.[12] In the present paper more detailed information on the generation and motion of defects in polymer crystals is obtained, with the goal to better understand the diffusion of chains through the crystal.

In the following section the methods and computational procedures used in this research are described. Then the results of the study are given, followed by a discussion and a summary of the conclusions.

Computational Methods and Procedures

It is important to note that dynamic disorder in a crystal involves large-amplitude, anharmonic motion. The motion of atoms under the influence of their anharmonic potential is, in addition, affected by dynamic processes such as kinetic and resonant coupling, dynamical barriers, and phase-space barriers. All of these processes have been shown to have significant effects on the kinetics and structure of molecular systems,[13-21] and quantum mechanical analogs of the classical observations have been demonstrated.[22-24] These types of dynamic processes are obviously important in any system which involves motion of particles under the influence of a potential and can be effectively studied using molecular dynamics.

The molecular dynamics method (MD) is well-known and has been reviewed in several recent papers.[25] Basically one needs to solve Hamilton's equations or any other formulation of the classical equations of motion starting from some initial positions and momenta of all the atoms in the system and propagate the solution in a series of time steps. In our MD simulations the integrations of the equations of motion are carried out in Cartesian coordinates, thus giving an exact definition of the kinetic energy. Integrations are performed using up to a 12th-order predictor/corrector routine with variable time steps. This method (ODE)[26] allows the integrations to be performed to a high accuracy. For example, conservation of all constants of motion (total energy, total angular, and linear momenta) is obtained to at least four digits without the need for any ad hoc scaling of the momenta.[4]

The molecular dynamics method requires the kinetic and potential energy of the system under study to be specified. We have used the following Hamiltonian:

$$H_{mol} = E_{kin} + \sum V_{2b} + \sum V_{3b} + \sum V_{4b} + \sum V_{Nb} \quad (1)$$

The potential functions for the adjacent bonded atoms

0024-9297/92/2225-7247$03.00/0 © 1992 American Chemical Society

are

$$V_{2b} = D\{1 - \exp[-\alpha(r_{ij} - r^\circ)]\}^2 \quad (2)$$

for the interaction between any two atoms not directly bonded together (1–4 types and larger)

$$V_{Nb} = 4\epsilon[(\sigma/r_{ij})^{12} - (\sigma/r_{ij})^6] \quad (3a)$$

or

$$V_{Nb} = A_{ij}\exp(-br_{ij}) - C_{ij}/r_{ij}^6 \quad (3b)$$

for the bending of a three-atom sequence

$$V_{3b} = {}^1/_2\gamma[\cos\theta_{ijk} - \cos\theta_0]^2 \quad (4)$$

and for the torsional coordinate τ between four successive atoms

$$V_{4b} = [8.37 + \alpha'\cos\tau_{ijkl} + \beta\cos^3\tau_{ijkl}] \quad (5)$$

The four-body potential term (eq 5) has two potential parameters (α',β)[27] which can be fitted to give a desired barrier height (for example, in polyethylene, a cis barrier of 16.7 kJ/mol and a gauche–trans energy difference of 2.5 kJ/mol). The constants D, α, and r° (see eq 2) represent the usual Morse oscillator parameters. The nonbonded terms ϵ and σ (eq 3a) represent the Lennard-Jones parameters, the exp-6 parameters A_{ij} and C_{ij} (eq 3b) are related to the overlap and dispersion of the atoms ij, and b is a parameter related to the position and well depth of the interaction. The bending force constant is γ, and θ_0 (eq 4) indicates the equilibrium value of the angle formed by the three atoms of interest in a particular bond. The potential energy parameters are given in Table I. The above potential energy functions (eqs 2–5) yield reasonably good spectroscopic, thermodynamic, and kinetic data as well as providing the atomistic details of temperature-dependent phase transitions for crystalline polymers.[3,5] They have been thoroughly tested over the past 5 years and provide a reasonable description for polyethylene. The reader is referred to our past publications for more details[3,5] and to an extensive link to prior and parallel literature with close to 100 references.[3]

We have examined the molecular dynamics of a model of a polyethylene crystal. The model is of the orthorhombic phase of polyethylene with unit cell dimensions a = 0.74 nm, b = 0.49 nm, and c = 0.26 nm. It consists of the 37 polyethylene (PE) chains containing 100 CH_2 groups each (oriented along the c axis) giving a crystal thickness of approximately 12.6 nm. Each PE chain lies initially on the lattice sites of the orthorhombic phase of polyethylene. The 37 PE chains are made up of 19 dynamic chains, surrounded by 18 static chains. The static chains consist of atoms that do not move during the simulation; i.e., while they keep a constant volume for the simulation, the dynamic chains do move. A constant pressure simulation has also been studied by eliminating the static chains.[3]

For the present calculations, we have chosen to collapse the CH_2 groups into a single particle of mass 14 amu. However, simulations with crystals containing up to 30 000 atoms that include the hydrogens explicitly are underway. The preliminary results, thus far, do not give any indications of being substantially different from the results or conclusions of the present study. Although the time scales and activation energies vary, the mechanisms remain unchanged (defect rate of formation per bond in the presence of hydrogens $\approx 2.5 \times 10^9$ s^{-1}; $E^* = 18.8$ kJ/mol). (These calculations require about 1 order of magnitude more CPU time than those without the hydrogens; i.e., completion of this project will take several years and selection of the simulations will be guided by the present results.)

Table I
Potential Energy Parameters for Equations 1–5

Two-Body Bonded Constants[a]	
D	334.72 kJ/mol
r_e	0.153 nm
α	19.1 nm^{-1}
Three-Body Constants[b]	
γ	130.122 kJ/mol
θ_0	113
Two-Body Nonbonded Constants[a]	
LJ 6–12 potential	
ϵ	0.494 kJ/mol
σ	0.39 nm
Exp-6 Potential[c]	
C	2236.81 kJ/mol
A	6.23853×10^5 kJ/mol
b	36.0 nm^{-1}
Four-Body Bonded Constants[a]	
α'	−18.4096 kJ/mol
β	26.78 kJ/mol

[a] Reference 27. [b] Weber, T. *J. Chem. Phys.* **1979**, *70*, 4277; **1970**, *69*, 2347. [c] Adapted from: Karaswa, N.; Dasgupta, S.; Goddard, W. A., III *J. Phys. Chem.* **1991**, *95*, 2260.

In all cases studied, the initial conditions of the simulations involve imparting a randomly chosen momentum, subject to a zero center-of-mass velocity constraint. Thus, the total added energy is initially purely kinetic. Due to the large number of atoms in the system, and thus the density of vibrational states, thermal equilibrium, as described by the standard Boltzmann distribution, is rapidly achieved. An effective temperature can then be determined by

$$E_{kin} = (3/2)Nk_BT = \sum[p_x^2 + p_y^2 + p_z^2]/(2m_i) \quad (6)$$

where k_B is Bolzmann's constant, T is temperature, and p and m are the Cartesian momenta and mass corresponding to atom i. In general, simulations were studied after allowing the kinetic energy to redistribute according to the dynamics of the system for 5 ps, thus giving both phase-averaged momenta and coordinates. This time has been found to be sufficient to reach a steady-state distribution as was clearly shown by time vs temperature plots[12] and is illustrated by the constancy of defect generation.[3]

In order to simulate a free energy gradient along the chain axis of the PE crystal, we have carried out two different kinds of calculations. In the first, the simulation of an overall "drag" force on the center PE chain was created by applying a constant external force to pull on the cylinder of six PE chains surrounding the center chain. This causes the six PE chains to move out of the crystal and produces an interaction force on the central chain. The interaction force has a net attractive component in the direction of the motion of the six surrounding chains, and a mean force on the center chain can be calculated. Thus, the effect of this simulation is to cause a "gradient force" on the center chain of the PE crystal of 37 chains.

A second method was to add to any defect in the center PE chain (recognized by having a $\cos\tau > 0$) a fixed, external force in the positive direction. This produces also a free energy gradient for motion in the chosen direction. An initial defect was created in the center chain by adding an appropriate kinetic energy pulse at positions 30 and 32 of the central chain, as discussed earlier.[3]

Both methods of introducing a free energy gradient yield the same minimum energy for a directed chain motion on

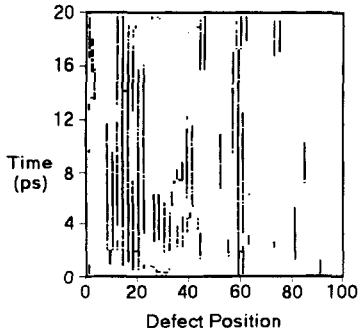

Figure 1. Plot of the defects generated in a model crystal (3700 CH_2 groups, 100 CH_2 groups per chain, in the orthorhombic phase of polyethylene) at T = 440 K. A defect is plotted by a ■ mark at the position of a torsion angle with a value of cos $\tau > 0.0$.

a 20-ps time scale. In a 12.6-nm-thick PE crystal it was determined to be approximately 4 kJ/mol at T = 350 K. Since both methods lead to similar results, we will focus the discussion of this paper on the results as a whole and not go into details of the differences of the two approaches.

In the molecular dynamics calculations, we have counted the number of times a classical trajectory uniquely passes through the transition state from the trans conformation in the direction of the neighboring gauche rotational isomer. The number of transitions that occur in the chains provides information on the number of rotational defects created during the simulation. In addition, from these data and the total time of the trajectory, the rate constant for isomerization and the activation energy can be determined using an equation derived from the transition state theory

$$\text{rate} = N_{st}(kT/h)e^{-E^*/kT} \quad (7)$$

where N_{st} is a statistical factor, E^* is the activation energy of the process considered, k and h are Boltzmann's and Plank's constants, respectively, and T is the temperature.

Lamellar thickening and defect motion was examined during the simulations by monitoring the positions of the ends of the PE chains along the c axis (direction of the PE chains), the end-to-end distance, and the positions of any generated defects. Plots of these quantities as a function of time give the necessary information to observe defect motion and chain diffusion. From these types of analyses, the mechanisms for the various processes can be determined.

Results

Typical snapshots of the motion of polymer crystals have been produced earlier[3] and can also be deduced from Figure 8 below. Movies have been presented at the 1990 and 1991 March Meetings of the American Physical Society.

A plot of the lifetime and location of defects for a simulation at high temperature without a free energy gradient to induce defect travel through the crystal in the central chain is shown in Figure 1. The solid lines indicate the life of a single gauche defect. Alternating black–white–black marks are representations of gauche–trans–gauche sequences. The creation of these types of defects requires an activation energy of about 16 kJ/mol (as determined by eq 7) and is thus possible at temperatures more than 100 K below melting (i.e., at room temperature). One can see the frequent clustering into kinks such as 2g1, which are known to be energetically more favorable than isolated gauche defects.[1] The symbol 2g1 represents the standard chain-defect nomenclature,[1] with 2g denoting the numbers of gauche conformations, and the second numeral, the

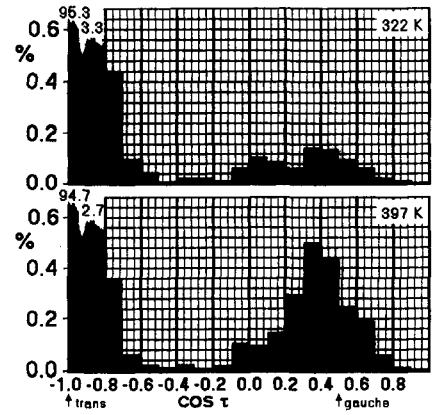

Figure 2. Histogram of the cosines of the torsional angle that occur during a 16-ps simulation at two different temperatures (T = 322 and 397 K). The angles corresponding to the trans and gauche conformations are marked in the figure for reference. The labels at the top of the histograms correspond to the percent of conformations at the two angles with off-scale amplitudes.

amount of shortening of the chain in multiples of $c/2$. In addition, there is a small lateral displacement. Typical rates for the formation per C–C bond of the conformational defects are 10^{10} s^{-1} at 350 K. Figure 2 illustrates the increase in the occurrence of defects with temperature as derived earlier [the conformational defects are counted as soon as the bond angle τ changes by more than 90° (cos $\tau > 0$) which exceeds the maximum in the potential energy for rotation (eq 5)].[3]

Figure 3 illustrates the change of the position of the bottom 30 CH_2 groups of a chain in the crystal as a function of time, again without a free energy gradient affecting the motion of the defect. The formation, life, and destruction of the defect can be seen to take about 3 ps in this example of a simulation at 320 K. To judge the chain rotation, the stationary initial positions of the chain segment are repeated in all three figures. From the distance of the chain from the tie lines, compression of the chain can be judged, and the direction of the chain end indicates when a 180° twist is present in the bottom segment.

Detailed analyses of the motion of defects through the crystals with a free energy gradient as discussed in the section on methods can be made from Figures 4–6 by combining the observation of gauche defect positions (a), the displacements of the chain ends (b), and changes in the end-to-end distances (c). Figure 4 shows data at 350 K for a crystal with 100 CH_2 group long chains. Figure 5 illustrates the same for a crystal with 50 CH_2 group long chains. Figure 6 refers again to a crystal with 100 CH_2 group long chains, but at a temperature of 238 K. The number of CH_2 groups that are removed by the given free energy gradient as a function of temperature and chain length are shown in Figure 7.

To see the fast motion of a soft, 180° twist in a crystal, a series of snapshots of a twist introduced before starting a simulation, followed in 0.5-ps intervals, is shown in Figure 8. Although this simulation is done at 50 K to exclude thermal gauche defects, the lifetime of the twist is less than 2 ps, as can be seen from the flip of the chain end. The distance traveled by the center of the defect is 3 nm; i.e., the speed of travel is 1.5 km/s, the order of magnitude of the sound velocity. More details on the relaxation of twist defects are given in ref 7a.

The final analyses involved the simulation of a polyethylene-like crystal which has two of the adjacent 100 CH_2 group chains in the center of the crystal connected by a fold. Figures 9 and 10 show the positions of the chain ends and the end-to-end distances for the case of a 4 kJ/

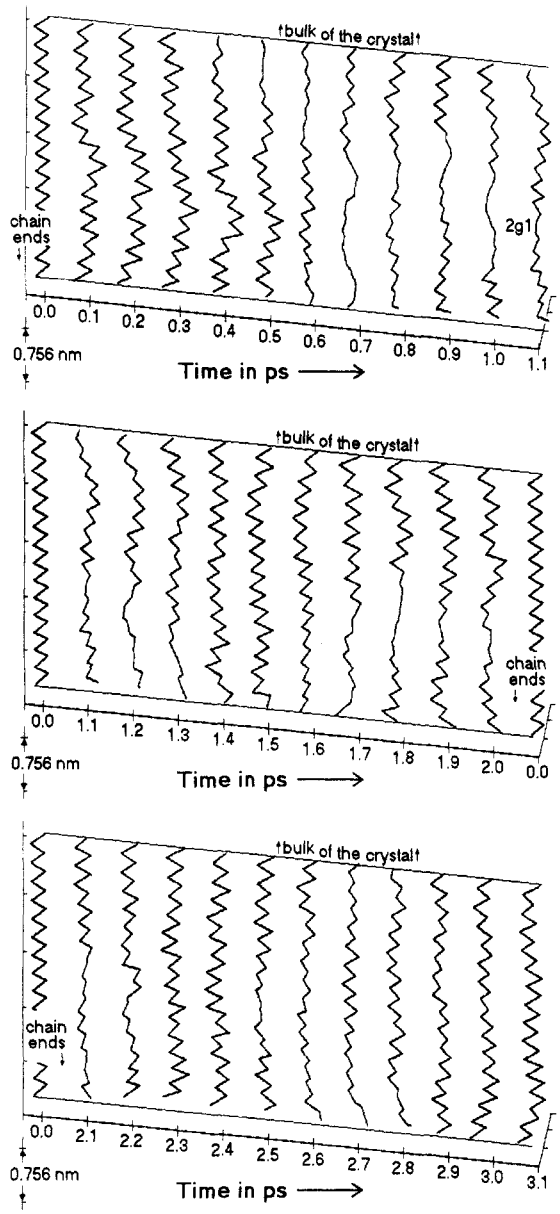

Figure 3. Time sequence of the x, y, and z positions of the bottom 30 CH_2 groups of a PE chain in the model crystal. x is parallel to the time axis, y, toward the back, and z, vertical in the chain-axis direction. The initial configuration of the PE chain (time = 0.0 ps) is plotted in each figure for reference. (a) For the time from 0 to 1.1 ps with the 2g1 position marked. (b) For the time from 1.1 to 2.0 ps. (c) For the time from 2.1 to 3.1 ps.

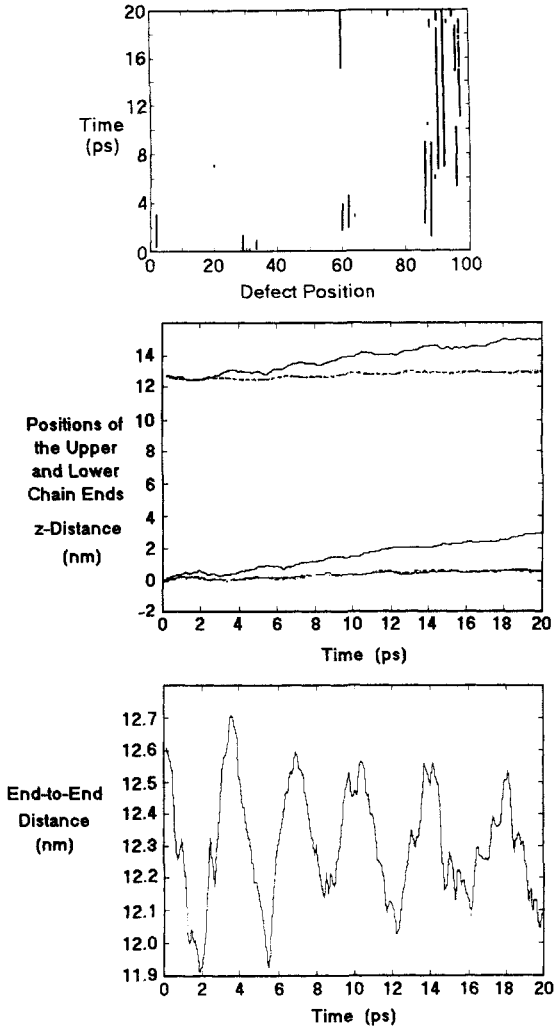

Figure 4. (a) Plot of the defects generated in the center chain as in Figure 1, except for a simulation in which a gradient force is applied on the crystal (T = 350 K). (b) Plot of the positions of the ends of the central PE chain along the chain axis (c axis) as a function of time. (The lines that are approximately at 0 and 12.6 nm are those for the surrounding PE chains that do not move.) (c) Plot of the end-to-end distance of the center PE chain as a function of time.

mol free energy gradient acting on one of the connected chains. In Figure 9 the gradient acts away from the fold, resulting in a transport through the fold while conserving position and size in the fold. In Figure 10 the gradient direction is reversed toward the fold. In this case the fold is pushed out of the crystal surface with a large decrease in the end-to-end distance.

Discussion

Many defects have been proposed for polymer crystals, often based on more or less extensive molecular mechanics calculations.[1] A more recent summary of basic defects[28] suggested interstitial-like and vacancy-like dispirations (extra or missing CH_2 group in the chain), interstitial dislocations (two extra CH_2 groups), and disclinations (two twists at constant chain length). All of these were computed to have a local energy minimum of 50–100 kJ/mol above the all-trans minimum. This compares to the heat of fusion of polyethylene of 4.1 kJ/mol. Additionally, all defects discovered by structure analysis such as edge and screw dislocations seem to be sessile and unsuitable to cause major mass transport, as is needed for annealing to a larger fold length or plastic deformation, as experienced by drawing or rolling.[1] In particular, there has never been a suggestion of a sufficiently active source of defects to feed a large deformation mechanism. The lifetime and concentration of thermal gauche defects shown in Figures 1 and 2 provide for the first time such a defect source. This enables the beginning of the development of a physics of the defect macromolecular crystal. Naturally, a single gauche defect cannot be introduced in a crystal without considerable strain along the chain and between chains. Inter- and intramolecular strains proved, however, to be much harder to be extracted from the results of our molecular dynamics simulation. Both are necessary to understand the details of the creation of defects, their lifetime, and their motion. A comprehensive model of defects should satisfy the following requirements:

1. There should be a mechanism for defect creation.
2. The energy for the creation and persistence of the defect should be relatively low.
3. The defects should have general applicability and not be structure specific.

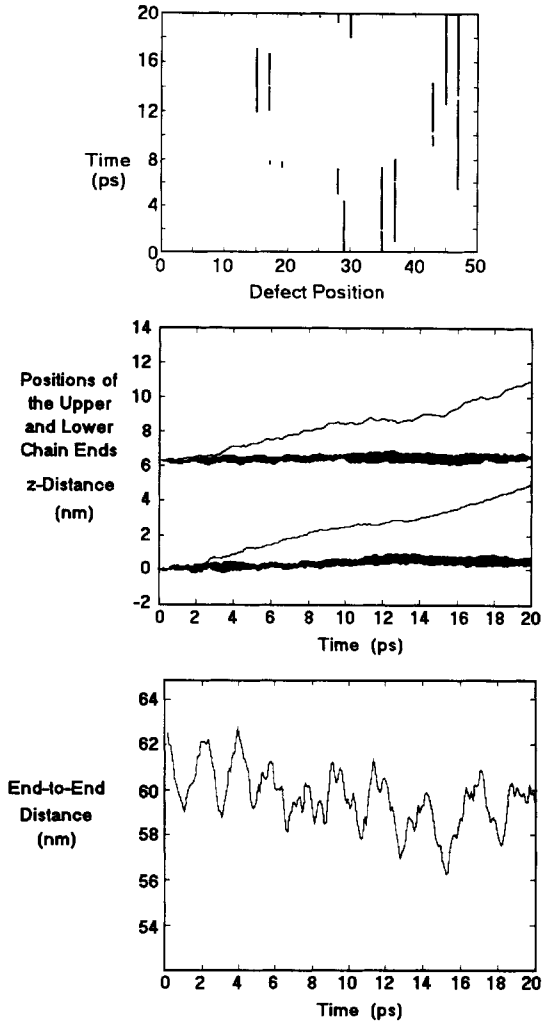

Figure 5. (a–c) Same as Figure 4, except for a PE crystal with chains of 50 CH_2 groups.

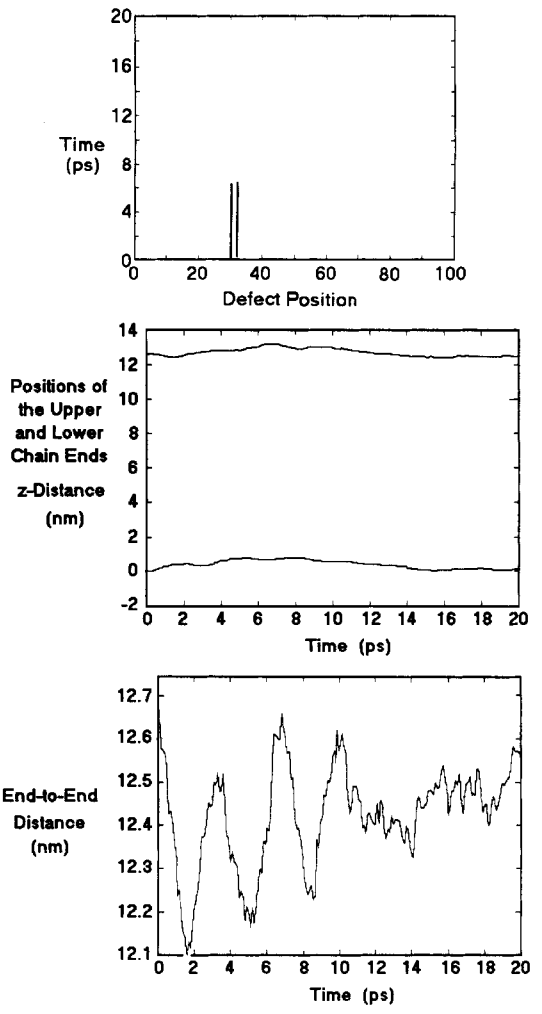

Figure 6. Same as Figure 4, except for a temperature of $T = 238$ K.

4. The defects should explain the observed relaxation in terms of mechanism and kinetics.

5. Mass transport in terms of the diffusion of the chain as observed in lamellar thickening and deformation must be accounted for.

6. The models must explain all experimental results (including those from vibrational spectroscopy, dynamic mechanical and dielectric analyses, calorimetry, X-ray diffraction, NMR relaxation time determinations, and dynamic neutron scattering).

Although far from a complete analysis, our molecular dynamics simulations point to solutions for all these points. Typical rates for the formation per C–C bond are 10^{10} s^{-1} at 350 K. The activation energy for the creation of the defects as derived from eq 7 is only 16 kJ/mol,[3] permitting the formation of substantial numbers of defects even 100 K below the melting temperature (see Figure 2). These two observations satisfy points 1 and 2 above.

The general applicability and a mechanism of the thermal defect formation can be gained from Figure 3. The chain displayed in the figure is at time zero approximately 45° rotated out of the plane of the paper which represents the crystallographic *ac* plane. After only 0.1 ps a clear transverse vibration, moving with a speed of about 2 km/s toward the chain end, becomes visible. After 0.4 ps a torsional vibration enters the top of the figure. A collision between the two brings about the creation of a twist defect, identifiable by a close to 180° twist of the last chain segment. The slight contraction of the chain is recovered shortly before the collision (0.6 ps). The

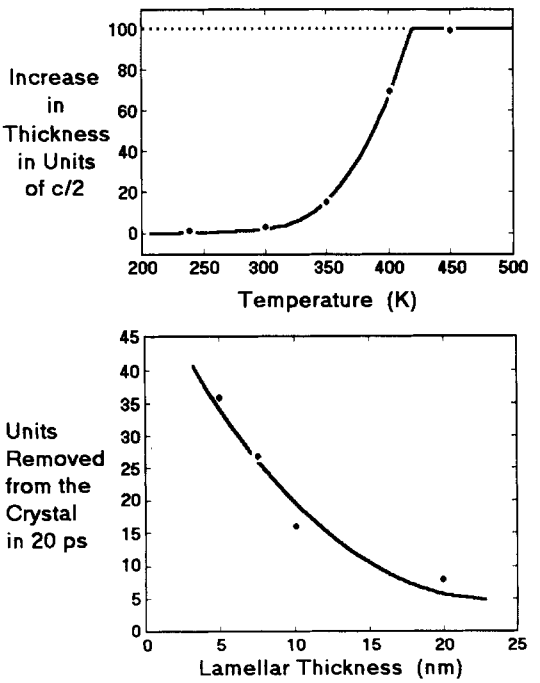

Figure 7. (a) Plot of the number of c/2 units that are removed from a model PE crystal with 100 CH_2 groups per chain in a time of 20 ps as a function of the temperature. (b) Same as Figure 7a except as a function of the crystal thickness and at a temperature of 350 K.

torsional vibration seems to be reflected at the chain end (0.7–0.9 ps) but is pinned by the mismatch of the chain

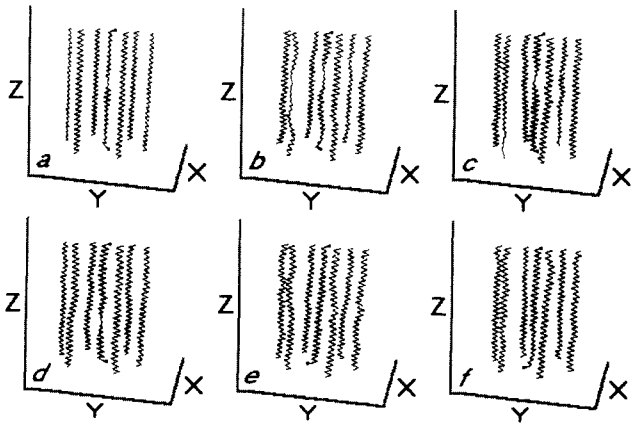

Figure 8. Plot of the configuration of the ends of seven PE chains in the crystal as a function of time at 50 K. (50 CH_2 groups out of the 100 of each chain are shown.) A soft twist defect is introduced initially between CH_2 groups 17 and 30 from the bottom. Subsequent pictures are in 0.5-ps intervals without a free energy gradient.

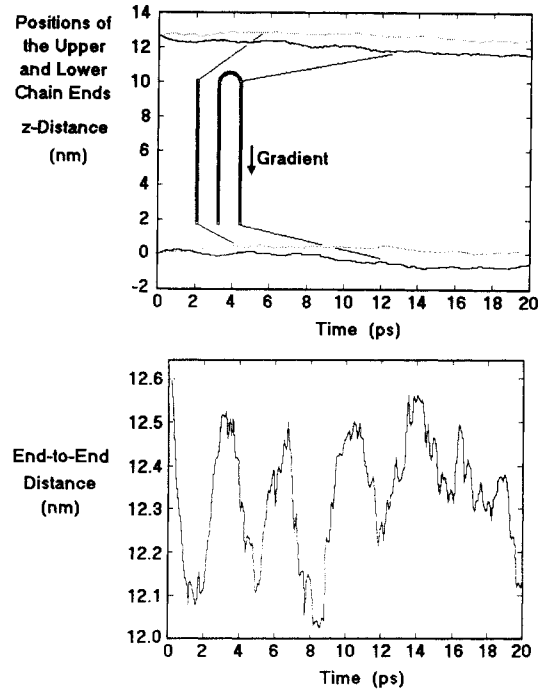

Figure 9. (a) Plot of ends of the center PE chain along the chain axis (c axis) as a function of time for a once-folded PE chain. A gradient is applied in the direction away from the fold. (b) End-to-end distance for one segment of the folded PE chain as a function of time. The temperature of the simulation was 350 K.

end. At 1.1 ps an approximate alignment of the last chain segment with the next higher (180° turned) lattice position can be seen. This situation should be similar to the interstitial-like dispiration;[28] i.e., an excess of at least 50 kJ/mol above the average must have been collected in the chain. By now the torsional vibration returns to the chain end, twists the chain in the opposite direction to the original, low-energy position at 1.4 ps, and gets reflected at 1.6 ps (with equilibrium chain length) to rotate the chain to a twist again (1.8 ps). At 2.3 ps the chain is shortened by about $c/2$ and has returned to a position without an obvious twist. Since in the projection an approximately 90° rotation about a bond cannot be seen, one must assume the formation of a 2g1 kink between CH_2 groups 9 and 13 from the end (2.2–2.5 ps). The final appearance of the torsional oscillation occurs between 2.6 and 2.8 ps with the disappearance of the kink and the

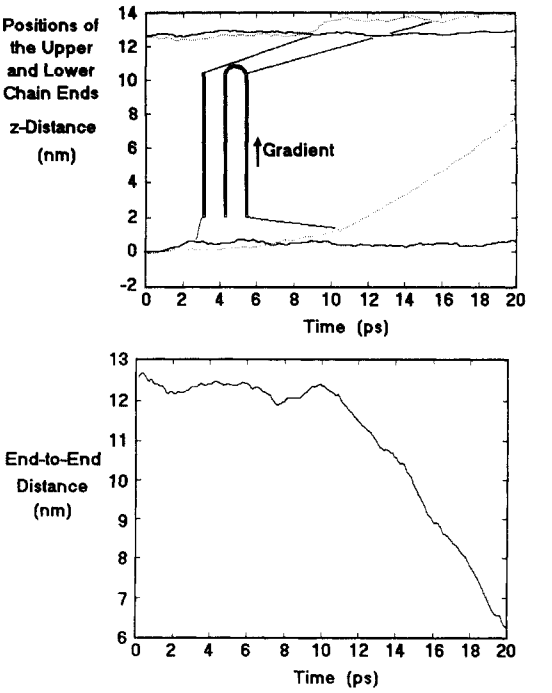

Figure 10. Same as for Figure 9, except that the gradient is applied in the direction toward the fold.

reappearance of a smaller transverse vibration at 3.1 ps and the equilibrium chain extension.

The description of the defect formation, life, and destruction will need further refinement by recording of other perspectives or detailed positions of CH_2 groups, not possible at present because of limitations of the computer memory. It shows, however, that a dynamic interaction of skeletal vibrations and defects exists that cannot be derived from molecular mechanics calculations.

In the time sequences of Figures 1 and 3 there is no motion of the defects toward either of the chain ends. After destruction of the defect no change in the crystal has occurred. In order to have mass transport that can lead to lamellar thickening or crystal deformation, a continuous stream of defects must move toward one end of the crystal. The direction of the travel is determined by any existing free energy gradient. For mechanical deformation the free energy gradient is caused by an external force.[10] Annealing is driven by the greater stability of a more extended chain crystal. It was suggested some time ago that the growth of lamellar thickness to large dimensions through chain diffusion involves conformational disorder.[29] Mesophases of large concentrations of conformational disorder (condis crystals) are seemingly always involved when extended-chain crystals[1] grow from a mobile melt. The only other mechanism to grow extended-chain crystals of flexible molecules is via crystallization during polymerization.[30,31] Since the time scale for a doubling of the crystal size is expected to be large relative to the present simulation times, we have chosen to assist the motion of the defects that are formed naturally. To achieve this, a gradient was placed on the crystal, as given in the Computational Methods and Procedures section. It effectively starts a mass transport down a potential barrier in the preferred direction. From the dynamics of the 3700 CH_2 group polyethylene-like crystal, an estimation of the activation energy needed for the motion that doubles the lamellar thickness on a 0.1-ns time scale was found to be 4 kJ/mol at T = 350 K (the activation energy decreases with decreasing lamellar thickness). Thus, once a sufficient population of defects has been generated by the dynamics of the crystal

(requiring an activation energy on the order of 16 kJ/mol as determined by eq 7), mass diffusion occurs down the chain in the direction of the free energy gradient.

Figure 4a shows the position of gauche defects, defined for bonds with a torsional angle of $\cos \tau > 0$ as a function of time. Twist defects cannot be seen in this representation but must be inferred from the movement of the chain as displayed in Figure 4b. The end-to-end distance of Figure 4c reveals a longitudinal acoustic vibration mode (LAM) of about 3×10^{11} Hz (10 cm^{-1}). Initially the chain is 12.6 nm long. Each 2g1 kink (sequence of gauche$^+$,trans,gauche$^-$ conformations) shortens the end-to-end distance by about 0.126 nm. Since at any time the number of gauche conformations in Figure 4a is about 4, the equilibrium distance of the end-to-end distance in Figure 4c is about 12.3 nm. As the chain diffuses through the crystal, the gauche defects collect toward the right and ultimately locate preferentially in the chain segment that is removed from the crystal. Every time the chain expands in the LAM vibration, it generates a sufficient number of twist defects to move 2 or 4 $c/2$ distances. Overall the center chain diffuses by about 16 $c/2$ units in five steps, interrupted by six contractions with negligible movement of the upper chain end in Figure 4b. The lower chain end, in contrast, shows somewhat more continuous motion, but marking the six maximum compression times from the LAM reveals that the compression pulls the chain end into the crystal. Overall, the center chain diffuses thus by six LAM contractions that pull the lower chain end into the crystal and five expansions that push the upper chain end out of the crystal by a total of 16 $c/2$ units in 20 ps. Perhaps it may be possible to link the creation of the twist defect with the abrupt changes in frequency and amplitude of the LAM superimposed on the overall vibration (see, for example, approximate times 0.5, 1.0, and 3 ps in Figure 4c). The other chains of the crystal remain without movement, as can be seen from Figure 4b. After about 100 ps the central chain is completely removed from the crystal, giving a measure of the time needed to double the lamellar thickness. The LAM is thus directly coupled to the reaction coordinate that leads to lamellar thickening. The additional influence of the transverse and twisting modes was illustrated in Figure 3.

The effect of lamellar thickness is documented for a crystal with 50 CH_2 groups in Figure 5. The total number of gauche defects is somewhat less (but more than half), so that the equilibrium length in Figure 5c is decreased from 6.3 to 6.1 nm initially and to about 5.9 mm at 20 ps, again in reasonable agreement with two or four gauche defects. The LAM frequency is increased at half the amplitude to about 19 cm^{-1}, in agreement with the expected 1/length dependence.[32] Because of the higher LAM frequency, the stepwise pulling of the chain into the crystal with contraction and expansion is less clearly seen in Figure 5b. In the 20 ps of the simulation, about 32 $c/2$ units were removed from the crystal, indicating a smaller activation energy of 2.8 kJ/mol for the smaller crystal. The larger number of twist defects moving the chain through the crystal is evident in the noisier LAM.

A summary of the temperature and lamellar thickness dependence of the mass transport process for a PE chain through the model crystal is shown in Figure 7. The number of $c/2$ units that are removed in 20 ps from a crystal with chains of 100 CH_2 groups is plotted as a function of temperature (Figure 7a), and the thickness dependence of the mass transport at $T = 350$ K is shown in Figure 7b. Increasing the temperature enhances the transport process, approximately obeying the transition state theory (eq 7), while increasing the lamellar thickness of the crystal decreases the number of $c/2$ units removed from the crystal. An Arrhenius plot can be extracted from these data and gives an activation energy for the process of $E^* = 17$ kJ/mol. This is near the value $E^* = 16$ kJ/mol determined from the transition state theory (eq 7) for the formation of conformational defects. The results shown in Figure 7b indicate that the rate of lamellar thickening as a function of the crystal thickness might be taken as approximately exponential [rate = $A \exp(-aL)$, where A and a are constants, and L is the crystal thickness]. Using this exponential relationship between the rate and crystal thickness and substituting it into eq 7 give an activation energy for the process which can be expressed in the form $E^* = C(L,T) + b(T)$ where $C(L,T)$ is the energy required to form a sufficient concentration of defects in a crystal of thickness L at temperature T, and $b(T)$ is related to the vibrational dynamics of the crystal. However, using this equation [where $C(L,T) = aL/kT$] will give a linear dependence of the activation energy on the lamellar thickness. As has been pointed out by Boyd,[28] this is not observed experimentally. If, on the other hand, we interpret Figure 7b to have a more linear dependence on L, then the activation energy would follow a dependence on L [$\approx -\ln(L/kT)$] that reaches an asymptotic limit for large L, as is observed experimentally.

The atomistic dynamics of the polymer crystal depicts thus that of a very chaotic system. However, it is interesting that the formation of other (perhaps less stable) defects can occur from the concerted effort of the motion and annihilation of thermal defects within the crystal and from their natural generation as was discussed for Figures 3–5. Figure 6 is a series of plots of the type discussed for Figures 4 and 5, but at a lower temperature ($T = 238$ K). In this case an initially introduced 2g1 defect (at positions 30 and 32) is stable for about 7 ps and subsequently does not move toward the edge of the crystal (Figure 6a). The equilibrium end-to-end distance is initially about 12.45 mm, as expected for one 2g1 kink. For the first three compressions and two expansions of the LAM, mass transport seems to proceed as in Figure 4. At 7 ps, coinciding with the destruction of the 2g1 kink, there is a change in the c-axis movement of the two ends of the PE chain (Figure 6b) and in the end-to-end distance (Figure 6c). After an additional 5 ps, at 11 ps of the dynamics, the LAM amplitude has been considerably reduced. The crystal gives the impression of being perfected and unable to support chain diffusion, noted by the stability of the end-to-end distance and the fact that the positions of the chain ends do not change. This observation seems to indicate that *without gauche defects no chain diffusion is possible*. That otherwise twist defects can move on fairly short time scales, even at low temperature, is shown in Figure 8, where an initially generated twist defect is rapidly quenched.[7] Additional support for the observation that thermal defects are necessary to have chain diffusion (that could lead to lamellar thickening) was obtained by repeating the simulation for Figure 6 without inducing the initial 2g1 defect. In this case the temperature is low enough that no thermal defects are induced naturally, and it is therefore a good control experiment for determining if thermal defects are the first step to a lamellar thickening process. Our observation clearly revealed that there was no chain diffusion, as opposed to the case presented in Figure 6 and more dramatically in Figures 4 and 5 where the thermal defect concentration was high.

In addition, a torsion-angle map was calculated for the angles $0 \leq \tau \leq 15$, $15 \leq \tau \leq 30$, $30 \leq \tau \leq 45$, etc., thereby giving relevant information on whether a 180° twist of the chain was formed. For the case of Figures 4 and 6, a twistlike defect was generated after about 2–5 ps, while there were none in the case where no thermal defects occur.

Finally, in order to assess the effect of folds in the polyethylene-like crystal, we have carried out the same simulations as described in Figures 4–6 for a once-folded polyethylene chain. The chain fold is placed at the top of the crystal. Figure 9 corresponds to a once-folded PE chain with a gradient energy (again, on the center chain only) of 4 kJ/mol, applied in the direction pointing away from the fold. This results in a diffusion of the folded chain while conserving the position and approximate size of the fold. The fold consists of a total of 7 CH_2 groups. The PE chains are effectively moved through the crystal as outlined in the discussion of Figure 4, while the end-to-end distance (distance along one side of the folded chain; Figure 9b) oscillates according to the frequency of the LAM. As discussed earlier, the change in the frequency of the LAM due to the formation of defects is observable in the plot of the end-to-end distance. The total amount that the folded chain is diffusing in 20 ps of dynamics is about 8 $c/2$ units, half as much as for the crystal without fold. Also note that one part of the chain is pulled outward, while the other is pulled inward. Overall, the effect of a fold on the internal dynamics for the process is, thus, not very significant; the chain passes easily through the folds. A mechanism that requires the fold to travel through the crystal, as was proposed by Dreyfuss and Keller[33] to explain annealing, would need simultaneous, parallel gradients on both chains connected at the fold.

If the gradient on the center chain is applied in the direction toward the fold, a different process is observed. This is shown in Figure 10 where there is a drastic change in both the position of the PE chain (Figure 10a) and the end-to-end distance (Figure 10b). In this case, the fold structure and position are drastically changed, effectively resulting in an amorphous-like region near its original position, thus causing the end-to-end distance and the c-axis position of the chain ends to change, as shown in Figure 10b. The motion is considerably enhanced over the case of Figure 9, removing more than half of the chain within 20 ps. The reason for the acceleration of the motion seems to lie in the increased number of defects created at the chain end and the shortening of the remaining crystallized portion.

Conclusions

For the first time a direct link seems to be established between the picosecond dynamics in a crystal and the chain motion needed for the macroscopic annealing and deformation. The process of chain diffusion in polymer crystals appears to occur via two steps. The first is the generation of a sufficient concentration of thermally caused gauche defects. These defects are frequently 2g1 and related kinks. The random-like formation of these thermal defects occurs on a picosecond time scale and requires an activation energy of approximately 16 kJ/mol for a crystal thickness of 12.6 nm (the activation energy is dependent on the lamellar thickness). The creation of the thermal defects leads to the formation of "larger", twist-like defects whose formation is also closely coupled to the skeletal vibrations of the crystal. An additional activation energy gradient of about 4 kJ/mol for a crystal of 12.6 nm thickness was found necessary to cause the doubling of the crystal thickness on a time scale of 0.1 ns. The overall defect motion leading to chain diffusion was shown to be temperature and lamellar thickness dependent, increasing with temperature and decreasing with lamellar thickness. Motion toward a fold creates an "amorphous" segment at the surface of the crystal, while motion away from the fold moves the chain through the fold that remains stationary.

Acknowledgment. This work was supported by the Division of Materials Sciences, Office of Basic Energy Sciences, U.S. Department of Energy, under Contract No. DE-AC05-840R21400 with Martin Marietta Energy Systems, Inc., and by the Polymer Program of the National Science Foundation, present Grant No. DMR-9200520. The computations were performed on the Cray YMP at the NSF Pittsburgh Supercomputing Center (Grant CHE910008P, Cray sponsored research) and the IBM 3090 at the University of Tennessee. We thank A. Xenopoulos for useful discussions.

References and Notes

(1) Wunderlich, B. *Macromolecular Physics; Crystal Structure, Morphology, Defects*; Academic: New York, 1973; Vol. 1.
(2) Annis, B. K.; Noid, D. W.; Sumpter, B. G.; Reffner, J. R.; Wunderlich, B. *Makromol. Chem., Rapid Commun.* **1992**, *13*, 169. Annis, B. K.; Wunderlich, B. *J. Polym. Sci., Part B: Polym. Phys.*, in press.
(3) Sumpter, B. G.; Noid, D. W.; Wunderlich, B. *J. Chem. Phys.* **1990**, *93*, 6875.
(4) Noid, D. W.; Sumpter, B. G.; Wunderlich, B.; Pfeffer, G. A. *J. Comput. Chem.* **1990**, *11*, 236.
(5) Noid, D. W.; Sumpter, B. G.; Varma-Nair, M.; Wunderlich, B. *Makromol. Chem., Rapid Commun.* **1989**, *10*, 377. Noid, D. W.; Sumpter, B. G.; Wunderlich, B. *Macromolecules* **1990**, *23*, 664.
(6) Roy, R.; Sumpter, B. G.; Noid, D. W.; Wunderlich, B. *J. Phys. Chem.* **1990**, *94*, 5720.
(7) (a) Noid, D. W.; Sumpter, B. G.; Wunderlich, B. *Macromolecules* **1991**, *24*, 4184. (b) Noid, D. W.; Sumpter, B. G.; Liang, G.; Wunderlich, B. *Proceedings of the SPE Meeting in Detroit*; SPE: Brookfield, CT, 1992, Vol. II.
(8) Wunderlich, B.; Xenopoulos, A.; Noid, D. W.; Sumpter, B. G. *Proc. 1990 Fall Meeting Mater. Res. Soc.* **1991**, *147*, Vol. 209.
(9) Noid, D. W.; Sumpter, B. G.; Wunderlich, B. Polymer Dynamics. *Adv. Polym. Sci.*, in press.
(10) Noid, D. W.; Sumpter, B. G.; Wunderlich, B. *Polym. Commun.* **1990**, *31*, 304.
(11) Sumpter, B. G.; Getino, C.; Noid, D. W. *J. Chem. Phys.* **1992**, *96*, 7072.
(12) Liang, G.; Sumpter, B. G.; Noid, D. W.; Wunderlich, B. *Makromol. Chem., Theory Simul.*, in press.
(13) Getino, C.; Sumpter, B. G.; Santamaria, J.; Ezra, G. S. *J. Phys. Chem.* **1989**, *93*, 3877.
(14) Noid, D. W.; Kozykowski, M. L.; Marcus, R. A. *Annu. Rev. Phys. Chem.* **1981**, *32*, 267. Noid, D. W.; Marcus, R. A. *J. Chem. Phys.* **1977**, *67*, 559. Noid, D. W.; Koszykowski, M. L. *Chem. Phys. Lett.* **1980**, *73*, 114. Noid, D. W.; Knudson, S. K.; Delos, J. B. *Chem. Phys. Lett.* **1983**, *100*, 367.
(15) McClelland, G. M.; Nathason, G. M.; Frederick, J. H.; Farley, F. W. In *Excited States*; Lim, E. C., Innes, K. K., Eds.; Academic: London, 1987; Vol. 7.
(16) Getino, C.; Sumpter, B. G.; Santamaria, J. *Chem. Phys.* **1991**, *145*, 1.
(17) Bondybey, V. E. *Annu. Rev. Phys. Chem.* **1984**, *35*, 591. Bloembergen, N.; Zewail, A. H. *J. Phys. Chem.* **1984**, *88*, 5459.
(18) Holme, T. A.; Hutchinson, J. S. *J. Chem. Phys.* **1985**, *83*, 2860. Hutchinson, J. S.; Hynes, J. T.; Reinhardt, W. P. *J. Phys. Chem.* **1986**, *90*, 3528.
(19) Lichtenberg, A. J.; Lieberman, M. A. *Regular and Stochastic Motion*; Springer-Verlag: New York, 1983. Oxtoby, D. W.; Rice, S. A. *J. Chem. Phys.* **1976**, *65*, 1676. Ford, J. *Adv. Chem. Phys.* **1979**, *24*, 155. Chirikov, B. V. *Phys. Rep.* **1979**, *52*, 265.
(20) Gray, S. K.; Rice, S. A.; Noid, D. W. *J. Chem. Phys.* **1986**, *84*, 3745. Mackay, R. S.; Meiss, J. D.; Percival, I. C. *Phys. D* **1984**, *13*, 55. Davis, M. J.; Gray, S. K. *J. Chem. Phys.* **1986**, *84*, 5389. Gray, S. K.; Rice, S. A.; Davis, M. J. *J. Phys. Chem.* **1986**, *90*, 3470. Davis, M. J. *J. Chem. Phys.* **1985**, *83*, 1016.

(21) Green, W. H.; Lawrence, W. D.; Moore, C. B. *J. Chem. Phys.* **1987**, *86*, 6000. Sumpter, B. G.; Martens, C. C.; Ezra, G. S. *J. Phys. Chem.* **1988**, *92*, 7193. Garcia-Ayllon, A.; Santamaria, J.; Ezra, G. S. *J. Chem. Phys.* **1988**, *89*, 801.
(22) Benito, R.; Borondo, F.; Kim, J.-H.; Sumpter, B. G.; Ezra, G. S. *Chem. Phys. Lett.* **1989**, *161*, 60. Martens, C. C.; Davis, M. J. *J. Phys. Chem.* **1988**, *92*, 3124. Waterland, R. L.; Min Yuan, J.; Martens, C. C.; Gillilan, R. E.; Reinhard, W. P. *Phys. Rev. Lett.* **1988**, *61*, 2733. Anchell, J. L. *J. Chem. Phys.* **1990**, *92*, 4342. Noid, D. W.; Koszykowski, M. L.; Marcus, R. A. *J. Chem. Phys.* **1979**, *71*, 2864. Noid, D. W.; Marcus, R. A. *J. Chem. Phys.* **1986**, *85*, 3305.
(23) Berry, M. V. *Phys. Ser.* **1989**, *40*, 335. Shapiro, M.; Goelman, G. *Phys. Rev. Lett.* **1984**, *63*, 1714. Gutzwiller, M. *J. Math. Phys.* **1971**, *12*, 343. Heller, E. *Phys. Rev. Lett.* **1984**, *53*, 1515.
(24) Channon, S. R.; Lebowitz, J. *Proc. N.Y. Acad. Sci.* **1980**, *357*, 108. Mackay, R. S.; Meiss, J. D.; Percival, I. C. *Phys. D* **1987**, *27*, 1.
(25) Klein, M. L. *Annu. Rev. Phys. Chem.* **1985**, *36*, 525. Hoover, W. G. *Annu. Rev. Phys. Chem.* **1983**, *34*, 103.
(26) Shampine, L. F.; Gordon, M. K. *Computer Solution of Ordinary Differential Equations: The Initial Value Problem*; Freeman: San Francisco, 1975. Shampine, L. F.; Gordon, M. K. DEPACK, SAND 79-2374.
(27) Sorensen, R. A.; Liam, W. B.; Boyd, R. H. *Macromolecules* **1988**, *21*, 194. Boyd, R. H. *J. Chem. Phys.* **1968**, *49*, 2574.
(28) Reneker, D. H.; Mazur, J. *Polymer* **1983**, *24*, 1387; **1988**, *29*, 3. See also the detailed discussion of twist defects in polyethylene by: Boyd, R. H. *Polymer* **1985**, *26*, 323, 1123.
(29) Wunderlich, B.; Grebowicz, J. *Adv. Polym. Sci.* **1984**, *60/61*, 1.
(30) Wunderlich, B. *Adv. Polym. Sci.* **1968**, *5*, 568.
(31) Wunderlich, B. *Macromolecular Physics, Vol. 2, Crystal Nucleation, Growth, Annealing*; Academic Press: New York, 1976.
(32) Mizoshima, S. I.; Shimanouchi, T. *J. Am. Chem. Soc.* **1949**, *71*, 1320.
(33) Dreyfuss, P.; Keller, A. *J. Polym. Sci., Part B* **1970**, *8*, 253.

Registry No. PE, 9002-88-4.